Available online at www.sciencedirect.com
ScienceDirect
Earth and Planetary Science Letters 261 (2007) 33–48
EPSL
www.elsevier.com/locate/epsl

Multiple events in the Neo-Tethyan oceanic upper mantle: Evidence from Ru–Os–Ir alloys in the Luobusa and Dongqiao ophiolitic podiform chromitites, Tibet

Rendeng Shi [a,b], Olivier Alard [c,d], Xiachen Zhi [a,*], Suzanne Y. O'Reilly [c], Norman J. Pearson [c], William L. Griffin [c], Ming Zhang [c], Xiaoming Chen [b]

[a] CAS Key Laboratory of Crust–Mantle Materials and Environments, School of Earth and Space Sciences, University of Science and Technology of China, 96 Jinzhai Road, Hefei, 230026, China
[b] State Key Laboratory of Mineral Deposit Research, Nanjing University, 22 Hankou Road, Nanjing, 210093, China
[c] GEMOC ARC National Key Centre, Department of Earth and Planetary Sciences, Macquarie University, Sydney, NSW 2109, Australia
[d] Géosciences Montpellier (CC 60), Université Montpellier 2, CNRS UMR 5243, 34095 Montpellier, France

Received 23 November 2006; received in revised form 21 May 2007; accepted 24 May 2007
Available online 31 May 2007
Editor: R.W. Carlson

Abstract

In situ analysis of major elements, platinum-group elements and Os isotope composition data for 170 grains of Ru–Os–Ir alloys from podiform chromitites in the Luobusa and Dongqiao ophiolites, Tibet, provide new constraints on the sources of the alloy grains, the Os-isotope composition of the Neo-Tethyan oceanic upper mantle, and the timing of melt–rock reactions in the ultramafic peridotites of the host ophiolites. Most alloy grains are osmiridium and iridosmine. Based on elemental and isotopic compositions, two populations can be identified. Group I, found in both ophiolite bodies, has fractionated PGE patterns typical of alloys and homogeneous $^{187}Os/^{188}Os$ 0.12645±4 (2s; $n=145$). Group II alloys from the Dongqiao ophiolites show smooth PGE patterns and $^{187}Os/^{188}Os$ ranges from 0.12003 to 0.12194 (yielding Re-depletion ages ≥1.1 Ga). Both the PGE patterns and the Os isotopic compositions of Group II resemble those of sulfides residual after melting.

Group I alloys represent an early cumulate phase during the crystallization of magmas and are interpreted as derived from an asthenospheric melt. In contrast, Group II alloys are inferred to derive from the breakdown of residual sulfides from the mantle section of the ophiolite, which may represent relics of a sub-continental lithospheric mantle. The coexistence of the two groups of alloys in Dongqiao samples reflects interaction between asthenosphere-derived melts and old depleted lithospheric mantle and suggests that the chromitites originated through melt–rock reactions. The data on the Group I alloys support the hypothesis that the Re–Os evolution of the convective oceanic mantle resembles that of enstatite chondrites.

Keywords: $^{187}Os/^{188}Os$ mantle composition; Ru–Os–Ir alloys; podiform chromitite; Luobusa ophiolite; Dongqiao ophiolite; Tibet

1. Introduction

Ophiolites are pieces of oceanic lithosphere that have been thrust onto the edges of continental plates; a

* Corresponding author. Tel.: +86 551 3607004.
E-mail address: xczhi@ustc.edu.cn (X. Zhi).

0012-821X/$ - see front matter © 2007 Elsevier B.V. All rights reserved.
doi:10.1016/j.epsl.2007.05.044

complete ophiolite section consists of mantle-derived peridotites, overlain successively by mafic and ultramafic lavas and sedimentary rocks such as greywackes and cherts. Based on comparisons of geochemical features with those of rocks from modern oceanic settings, they can be classified into ophiolites formed at divergent plate boundaries (mid-oceanic ridges; MOR-type) and at convergent plate boundaries (supra-subduction zones; SSZ-type). The peridotitic part of ophiolite sections is usually interpreted as the refractory residue remaining after extraction of basaltic melt at spreading centres. Chromitite bodies commonly occur within the ophiolitic mantle peridotites.

Ophiolitic chromitites represent one of the major types of chromite deposits, and include both podiform and banded types. Podiform chromitites are significant in understanding the processes that generate and modify lithospheric mantle; they are economically important, but poorly understood. On the basis of the $Cr^{\#}$ (Cr/(Cr+Al)) of chromite, the podiform chromitites are subdivided into Cr-rich and Al-rich types, interpreted as formed in SSZ or at mid-ocean ridges, respectively. They usually are situated near the crust–mantle boundary in such sequences (e.g. Lago et al., 1982). Most occurrences appear to be associated with dunite, representing former melt channels in harzburgite or lherzolite (e.g. Zhou et al., 1996). Their mechanism of formation is still controversial, with debate centred around 4 major models. 1) Early models interpreted the host rocks as magmatic, and thus considered that the chromitite crystallized from ultramafic magmas, like the banded chromitites found in cumulate rocks (Lago et al., 1982). 2) Another early model interpreted the chromitite as the residue of partial melting in the upper mantle, and thus as a member of the residual peridotite suite (Dick and Bullen, 1984). 3) More recently, it has been proposed that ophiolitic chromites (especially podiform chromitite) are related to the crystallization of mantle-derived partial melts, through melt–rock or melt–melt interaction near the crust–mantle boundary (Zhou et al., 1996; Ballhaus, 1998). Finally, 4) the presence of unusual mineral assemblages (Ru–Os–Ir alloys, SiC, native Fe, FeO, diamond) and coupled high $^{186}Os/^{188}Os$ and $^{187}Os/^{188}Os$ have been used to argue that the chromitites are derived from the core–mantle boundary (Bai et al., 2000; Robinson et al., 2004).

In addition to olivine and Si-rich melt inclusions, the chromite commonly contains tiny inclusions of platinum group minerals (PGM), e.g. Osmiridium, Ruthenoiridosmine, Erlichmanite or Laurite, which control the Os budget of the chromitites. Due to their refractory nature and high Os concentrations, Os-rich PGE alloys are robust representatives of the reservoirs from which they are derived. Furthermore, the extremely resistant nature of chromite provides an efficient shielding (armor) for the chromite-hosted PGM, ensuring that their Os isotopic composition has not been altered by "late secondary" processes. Finally, the very low Re/Os ratios of the Ru–Os–Ir alloy phases, coupled with their high Os concentrations, mean that only limited age corrections are required to obtain initial Os isotopic compositions. These features make chromites and associated alloy phases ideal material to investigate the Os isotopic composition and evolution of the convective upper mantle and/or to quantify the geochemical heterogeneity of this reservoir through time (Hattori and Hart, 1991; Walker et al., 2002a; Meibom and Frei, 2002; Meibom et al., 2002; Meibom et al., 2004; Malitch, 2004; Walker et al., 2005; Frei et al., 2005; Ahmed et al., 2006).

In this paper we present compositional data and *in situ* Re–Os analyses of Ru–Os–Ir alloy grains enclosed in chromitites from the Luobusa ophiolites in the Yarlung–Zangbo suture (Southern Tibet) and the Dongqiao ophiolites in the Bangong–Nujiang suture (Northern Tibet). The Os isotopic composition of chromite and associated PGMs, and their relationship to the convective upper mantle, cannot be interpreted in isolation; the chromites and the PGM are genetically related. We therefore discuss the mechanism of podiform chromitite formation and the origin of the related Os–Ir-rich alloys based on the composition and Re–Os isotopic characteristics of those alloys. We will demonstrate that 2 groups of alloys can be recognized, with different compositional trend and contrasted Os isotopic composition, representing two distinct mantle reservoirs. The coexistence of these two groups of alloys provides strong constraints on the origin of the PGMs and their host chromites.

2. Geological background and samples

2.1. Geological background

The Luobusa and Dongqiao ophiolites lie along two major belts delineating important suture zones in the Tibetan plateau (Fig. 1). The Yarlung–Zangbo suture in the south marks the boundary between the Indian subcontinent and the Lhasa block, whereas the Bangong–Nujiang suture in the north separates the Lhasa block from the Qiangtang block (Allègre et al., 1984). The Luobusa ophiolite lies within the Yarlung–Zangbo suture zone about 200 km ESE of Lhasa city; it represents a well-preserved and comprehensive sequence of obducted lithosphere (Fig. 1). The Dongqiao

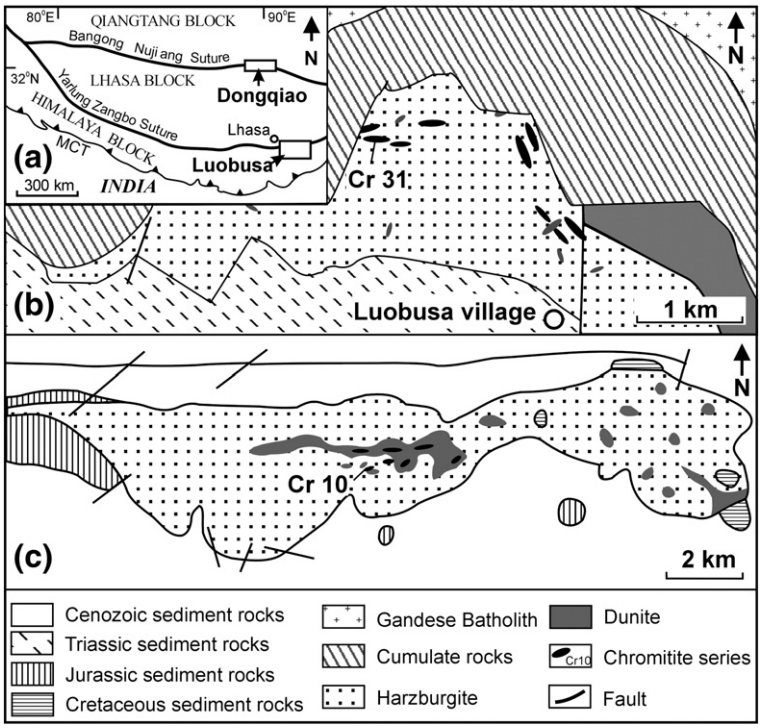

Fig. 1. a, Structural framework of Tibet and adjacent India, showing position of the Luobusa and Dongqiao ophiolites. MCT: Main Central Thrust; MBT: Main Boundary Thrust. Maps of the sample areas: b, Luobusa ophiolite, with position of the #31 chromite ore body; c, Dongqiao area, showing position of the #10 chromite ore body.

ophiolite, located about 500 km north of Lhasa city, forms a large, well-preserved section in the Bangong–Nujiang suture zone. It lies in a key location at the inferred junction between the eastern and western Neo-Tethyan domains (Fig. 1). The ophiolites consist of mantle peridotites, cumulate gabbros and pillow lavas inferred to represent the Neo-Tethyan oceanic lithosphere formed during the breakup of the Gondwana supercontinent, which had aggregated during the Pan-African tectonic event (Sengor, 1984).

The Luobusa ophiolite consists of fault-bounded slabs, approximately 1–2 km thick. To the north, these blocks are thrust over the Tertiary Luobusa Formation and the Gangdes granitic batholith; to the south, they are separated from Triassic flysch by a steep reverse fault (Fig. 1). The pillow lavas include major island-arc tholeiites (IAT) and minor MORB; cumulates comprise dunite, wehrlite, and pyroxenite with minor plagioclase, and the mantle peridotites are dominantly harzburgite with minor dunite and lherzolite. The Luobusa and Dongqiao ophiolites are correlated with coeval ophiolites that mark the opening of the Neo-Tethyan Ocean and the breakup of the early Paleozoic Gondwana continent between Permian and Triassic time (≈210–280 Ma (Sengor, 1984)). The Luobusa ophiolite is believed to have formed in two stages. Stage 1 is represented by MORB-type lavas and gabbroic dikes; whereas stage 2 is represented by the intrusion of boninites and a swarm of gabbroic dykes that locally crosscut the chromitite pods, and may be related to the formation of the chromitites by melt–rock reaction (model 3, above (Malpas et al., 2003)). A Sm–Nd isochron for two whole rocks and plagioclase and clinopyroxene separates from a Stage 2 gabbroic dyke yielded an age of 177±31 Ma (Zhou et al., 2002). Ar–Ar dates on amphibolites from the mélange zone range from 90 to 80 Ma and are interpreted as the age of intra-oceanic thrusting (Malpas et al., 2003). Final exhumation and emplacement probably took place in Early Neogene time (Malpas et al., 2003).

In the Dongqiao area, the mantle sequence lies in the centre of the belt and is 17.5 km long by 2–4 km wide (Fig. 1). The ophiolite blocks are thrust over a thick series of Middle Jurassic sandstones and black slates, and are structurally overlain by a nappe of Paleozoic metasedimentary rocks. Emplacement of the Dongqiao ophiolite is thought to have occurred during Late Jurassic time because the ophiolite is covered transgressively by subaerial to shallow marine latest-Jurassic sedimentary rocks (Allègre et al., 1984). A mid-Jurassic K–Ar age of ca 196 Ma has been obtained for the

Table 1
Major-element composition of chromites from the Luobusa and Dongqiao podiform chromitites (Data from Bai et al., 2000)

	Al_2O_3	FeO_T	Cr_2O_3	MgO	Cr#	Mg#
Luobusa						
Max.	15.14	17.93	61.98	16.67	0.80	0.79
Min.	8.83	12.75	45.69	13.14	0.77	0.62
Dongqiao						
Max.	19.24	16.06	59.89	16.43	0.80	0.75
Min.	9.85	12.52	50.51	13.27	0.70	0.60

metamorphic sole, several meters thick, that underlies the Dongqiao ophiolite (Zhou et al., 1997).

2.2. Samples

In both the Luobusa and Dongqiao ophiolites, the chromitites occur as tabular, lenticular and podiform bodies in the depleted harzburgites near the boundary with the massive dunites. Most chromitites are surrounded by envelopes of dunite. The chromitites lie at a relatively uniform depth within the mantle section, suggesting the formation of numerous pockets of melt accumulation at the point where mantle flow changed from vertical to horizontal.

Chromite from Luobusa and Dongqiao shows similar composition. Cr# of spinel ranges between 0.77 and 0.80 in the Luobusa chromitite, and between 0.70 and 0.80 in the Dongqiao chromitite. Chromite Mg# ranges between 0.62 and 0.79 in the Luobusa body and between 0.60 and 0.75 in the Dongqiao chromitites (Table 1; Fig. 2). In Cr# vs Mg# space both the Luobusa and Dongqiao chromites overlap the field of spinels from boninites. The range of chromite composition is restricted to high Cr# values, in contrast to what is observed in some other bodies such as the Oman Ophiolites (Rollinson, 2005) (Fig. 2).

Numerous grains of alloy phases containing platinum group elements (PGE) and base metals were separated (see Analytical methods, below) from the podiform chromitites. These include Os–Ir, Ru–Os–Ir, Pt–Fe, Ir–Ni–Fe, Fe–Cr–Ni and Fe–Co with highly variable compositions. Detailed petrographic observations show that most grains of Os–Ir alloys are enclosed in chromite and are not connected to fractures, and therefore must be considered as primary. These are mostly subhedral to anhedral, equidimensional grains up to 0.5 mm in diameter; most of them are monophase but Os–Ir and Ir–Os phases may be intergrown. More detailed descriptions of the Ru–Os–Ir alloys and other inclusion mineral assemblages are given by Bai et al. (2000).

3. Analytical techniques

Grains of Ru–Os–Ir alloys were separated from about 1500 kg of chromitite from orebody #31 in the Luobusa ophiolite and about 1000 kg of chromitite from orebody #10 in the Dongqiao ophiolite. Mineral separation was carried out at the Institute of Multipurpose Utilization of Mineral Resources, Zhengzhou, China, using a combination of vibration, magnetic, flotation and electronic conductivity techniques (Bai et al., 2000). The separation yielded 150 alloy grains from the Luobusa ophiolite and 20 from the Dongqiao ophiolite. The hand-picked Ru–Os–Ir alloy grains were mounted in epoxy and machine polished.

The Ru–Os–Ir alloys were analyzed by electron microprobe (EMPA) at Nanjing University using a JEOL-JXA 8800 automated microanalyzer with a sample current of 10 nA and an accelerating potential of 20 kV with a beam diameter of about 1 μm. Counting time was 100 s on peak and 20 s on background. The following X-ray lines were used: RuLa, RhLa, PdLh, OsMa, ReLa, IrLa, PtLa, NiKa; native elements were used as standards.

In situ Re–Os isotopic analyses of the alloys were carried out at the GEMOC ARC National Key Center,

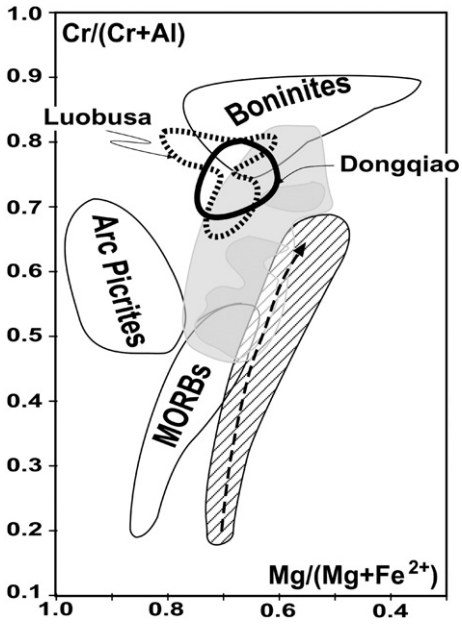

Fig. 2. Compositional field for chromites from Dongqiao and Luobusa Ophiolites (solid bold line and dashed bold line, respectively), compared with chromite composition field for Mid-ocean ridge basalts (MORBs), arc picrites and boninites (see Rollinson, 2005) and references there in). Also shown are chromite compositions from the Oman chromitites (gray area, (Rollinson, 2005) and references there in) and Oman harzburgites (stippled area).

Table 2
Elemental and Re–Os isotopic composition of the Os-rich alloys from Luobusa and Dongqiao

Spot		Ru	Ir	Rh	Pd	Pt	Os	Re	Total	Re/Os	Os/Ir	Pd/Ir	$^{187}Re/^{188}Os$	1SE	$^{187}Os/^{188}Os$	1SE	T_{RD} (Ma)					
																	ECR		PUM		CHUR	
Luobusa ophiolite, Southern Tibet																						
112	Max.	0.52	62.2	0.13	0.04	0.76	34.9	0.25	98.77	0.0072	0.562	0.0006	0.00011	0.00003	0.12672	0.00006	196.4	8.8	428.6	9.2	41.8	9.3
	Min.	0.49	62.1	0.09	0.09	0.65	37.2	0.15	100.80	0.0040	0.598	0.0015	0.00061	0.00009	0.12624	0.00006	264.0	8.7	499.2	9.0	112.8	9.1
113	Max.	0.22	67.9	0.05	0.03	2.18	30.2	0.12	100.73	0.0041	0.444	0.0004	0.00104	0.00005	0.12671	0.00004	198.1	6.3	430.4	6.5	43.6	6.6
	Min.	0.74	41.6	0.03	0.06	0.24	58.1	0.20	100.97	0.0035	1.396	0.0014	0.00022	0.00002	0.12620	0.00004	270.4	5.1	505.9	5.3	119.5	5.4
114	Max.	1.23	62.0	0.31	0.14	1.39	35.6	0.21	100.89	0.0060	0.575	0.0023	0.00030	0.00004	0.12623	0.00003	266.5	4.7	501.7	4.9	115.3	4.9
	Min.	0.67	42.3	0.10	0.01	0.44	55.8	0.14	99.45	0.0026	1.318	0.0002	0.00019	0.00002	0.12666	0.00003	205.4	3.7	438.0	3.9	51.2	3.9
13	Max.	1.38	41.3	0.00	0.08		55.3	0.26	98.34	0.0047	1.338	0.0019	0.00026	0.00004	0.12622	0.00004	268.2	5.4	503.5	5.6	117.1	5.7
	Min.	3.13	42.1	0.14	0.14	0.25	53.5	0.15	99.44	0.0028	1.269	0.0033	0.00014	0.00004	0.12668	0.00005	202.0	6.4	434.4	6.7	47.6	6.7
Average													0.00036	0.00004	0.12646	0.00004	233.9	6.1	467.7	6.4	81.1	6.4
Dongqiao ophiolite, Northern Tibet																						
20	Max.	33.03	25.3	2.55	2.26	4.31	31.0	0.07	98.47	0.0023	1.225	0.0893	0.00056	0.00005	0.12616	0.00005	275.8	7.4	511.5	7.7	125.2	7.8
	Min.												0.00044	0.00004	0.12636	0.00005	247.6	6.8	482.0	7.1	95.5	7.2
27	Max.	0.60	60.6	0.10		0.89	37.7	0.19	100.02	0.0050	0.622	0.0000	0.00018	0.00004	0.12654	0.00004	221.6	5.0	454.9	5.2	68.2	5.2
	Min.	0.37	61.6	0.17	0.12	1.19	37.5	0.13	101.12	0.0035	0.608	0.0019	0.00035	0.00004	0.12632	0.00003	253.2	4.5	487.9	4.7	101.5	4.8
28	Max.	1.96	42.3	0.22	0.12	0.34	54.0	0.16	99.13	0.0029	1.275	0.0029	0.00024	0.00003	0.12636	0.00004	247.9	5.0	482.3	5.2	95.8	5.2
	Min.	2.20	43.8	0.15	0.08	0.34	53.8	0.33	100.77	0.0061	1.228	0.0019	0.00019	0.00001	0.12664	0.00003	208.4	3.7	441.1	3.9	54.3	3.9
Average													0.00033	0.00003	0.12640	0.00004	242.4	5.4	476.6	5.6	90.1	5.7
14(1)	Max.	45.63	19.7	1.50	2.22	1.90	29.0	0.01	99.97	0.0003	1.472	0.1128	0.00082	0.00007	0.12047	0.00008	1078	11	1349	12	968	12
	Min.	33.90	15.2	0.97	1.38	3.41	45.3	0.01	100.17	0.0002	2.969	0.0905	0.00032	0.00003	0.12194	0.00003	871.3	4.6	1132.8	4.8	750.5	4.9
20	Max.	45.63	19.7	1.50	2.22	1.90	29.0	0.01	99.97	0.0003	1.472	0.1128	0.00062	0.00004	0.12148	0.00005	937.2	6.6	1201.5	6.9	819.6	6.9
	Min.	0.15	3.0	1.38	0.60	77.37	0.1		82.63	0.0000	0.044	0.2037	0.00133	0.00009	0.12003	0.00005	1139.3	7.4	1412.2	7.7	1031.7	7.8
29	Max.	13.19	37.7	0.65	0.68	2.52	43.9	0.05	98.76	0.0012	1.164	0.0180	0.00002	0.00006	0.12123	0.00006	971.7	7.7	1237.5	8.0	855.9	8.1
	Min.	13.19	37.7	0.65	0.68	2.52	43.9	0.05	98.76	0.0012	1.164	0.0180	0.00020	0.00003	0.12106	0.00004	995.4	5.2	1262.2	5.4	880.7	5.4
Average													0.00055	0.00005	0.12104	0.00005	998.9	7.1	1265.8	7.5	884.3	7.5

Department of Earth and Planetary Sciences, Macquarie University, using a laser ablation microprobe (LAM) attached to Nu Plasma multi-collector inductively coupled plasma mass spectrometer (MC-ICPMS) in the Geochemical Analysis Unit, GEMOC National Key Centre, Macquarie University. The LAM was a New Wave Research UP213 system, which has an Nd: YAG laser with a fundamental wavelength of 1064 nm and uses harmonic generators to produce a monochromatic beam of 213 nm. The operating conditions for the laser included a repetition rate of 2 Hz, an energy density of approximately 4.5 mJ/cm^2 (measured in a beam splitter) and an aperture size of 15 μm. Ablation of the sample was carried out in pure He (~0.9–1.0 l/min) and the sample/He aerosol was mixed with Ar (0.6 to 0.7 l/min) prior to introduction into the ICP. The mass spectrometer setup follows the method described in Pearson et al. (Pearson et al., 2002). Since that work was published NU005 has been upgraded with a stainless steel interface and the EM28 rotary pump has been replaced with an Edwards EM2-80 pump on the interface. All measurements were made in static mode using Faraday cup collectors. In addition to the Os isotopes, potential isobaric interferences from Pt, Re and W were monitored. This combination of masses resulted in the following cup configuration: ^{194}Pt (H6), ^{192}Os (H5), ^{190}Os (H4), ^{189}Os (H3), ^{188}Os (H2), ^{187}Os (H1), ^{186}Os (Ax), ^{185}Re (L1), ^{182}W (L3). Experiments on solutions show that the Re overlap can be reliably corrected up to a ^{187}Re/^{188}Os ratio of 1.60 (Pearson et al., 2002). All measurements were made in the time-resolved data collection mode. The background was measured on the gas blank for 30 s at a half-mass offset, with no ESA deflection. After the background measurement the laser was then fired and the signal was collected for 120 to 150 s. Corrections for mass bias used the exponential law and a normalization value for ^{189}Os/^{192}Os = 0.39593.

4. Major-element composition of alloys

The major-element compositions of the Ru–Os–Ir alloys are given in Table 2 and Fig. 3.

4.1. Luobusa ophiolite

In the Luobusa sample, the alloys are mainly composed of Os and Ir with minor Ru. Os and Ir contents vary between 36.2 and 70.4 wt.%, and between 29.8 and 67.9 wt.%, respectively, while Ru ranges between 0.1 and 4.4 wt.% The Os contents are bimodal, with peaks on each side of the osmiridium–iridosmine miscibility gap at ≈30–40 wt.% and 50–60 wt.%, corresponding to Ir contents of ≈58–70 wt.% and 38–45 wt.%, respectively. In the nomenclature of Harris and Cabri (1991), they comprise osmiridium and iridosmine. The primitive mantle (PM)-normalized PGE patterns of the Luobusa Os-rich alloys are characterized by a stepped profile due to strong fractionation between the PGE (Fig. 3). These patterns show extremely high Os and Ir but low abundances of Ru, Rh, Pt and Pd (Fig. 3). The Re contents are also low, ranging from 0.08 to 0.25 wt.%, yielding Re/Os between 0.0020 and 0.0046, much lower than the chondritic value (0.08).

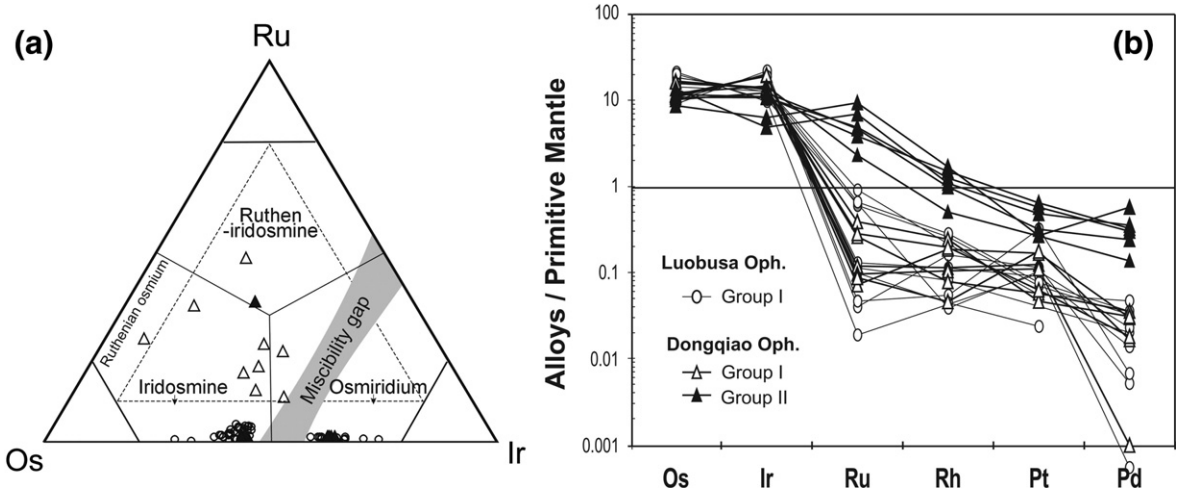

Fig. 3. a, Compositions of the analyzed alloy grains from the Luobusa and the Dongqiao ophiolites in Os–Ir–Ru space, with fields from Harris and Cabri (1991). Note the two groups for Dongqiao Os-rich alloys, Group I with low Ru, and Group II with high Ru grains. b, Primitive-mantle-normalized PGE concentrations of Group I and Group II alloys from Luobusa and Dongqiao.

In the Dongqiao sample, two distinct populations of alloys are recognized, hereafter dubbed Group I and Group II. Group I resembles the alloys described from Luobusa (Fig. 3). They are osmiridium and iridosmine (Harris and Cabri, 1991) with Os and Ir ranging between 36.2–55.3 wt.% and 42.3–61.6 wt.% respectively; the two elements show a bimodal distribution on either side of the miscibility gap (Fig. 3). Low abundances of Ru, Rh, Pt and Pd characterize Group I alloys, and they have the same stepped PM-normalized PGE pattern as the Luobusa alloys (Fig. 3).

The Dongqiao Group II alloys show similar high Os concentrations ($29 \le Os \le 60$ wt.%) but much higher Ru contents ($11.4 \le Ru \le 45.6$ wt.%) and trend toward Rutheniridosmine and Ruthenian Osmium compositions (Fig. 3). The most distinctive characteristic of Group II alloys relative to Group I alloys is their smooth PM-normalized PGE patterns, which show a continuous decrease from the highly refractory PGE (Os, Ir, Ru) toward the less compatible PGE (Rh, Pt, Pd) (Fig. 3). Although Rh, Pt and Pd show low abundances relative to Os, Ir and Ru, they are higher than in Group I alloys. Therefore Group II alloys show distinctive Pd/Ir (0.01–0.12), much higher than in the Group I alloys ($Pd/Ir \le 0.003$ in both localities). The Re contents of Dongqiao Group I and Group II alloys are low, ranging from 0.01 to 0.33 wt.% and yielding Re/Os well below the chondritic value, as in the Luobusa grains.

5. Osmium-isotope characteristics

The Re–Os isotopic compositions of the Group I and Group II alloys from the Luobusa and Dongqiao podiform chromites are presented in Table 2 and Fig. 4.

5.1. Luobusa ophiolite

The $^{187}Os/^{188}Os$ in the Group I Ru–Os–Ir alloys ranges from 0.1262 to 0.1267 with an average $^{187}Os/^{188}Os$ value of 0.12645 ± 0.00004 (2σ, $n=145$,

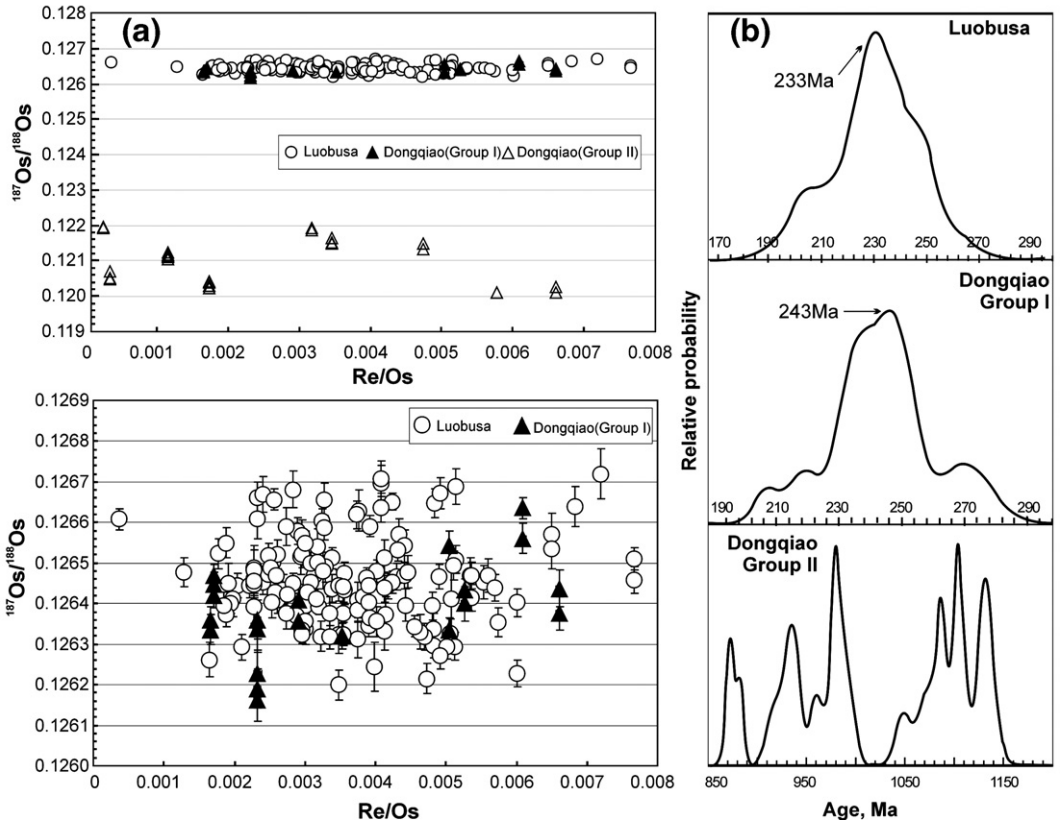

Fig. 4. Relations between Os-isotope composition and elemental composition in the analyzed alloy grains. a, $^{187}Os/^{188}Os$ vs Re/Os. The upper panel shows the lack of correlation between Re/Os and Os-isotope composition in the two groups of alloys in the Dongqiao sample. b, $^{187}Os/^{188}Os$ vs Ru contents. The compositional difference observed between Group I and Group II is coupled with an isotopic difference, Group II alloys from Dongqiao have high Ru contents and low $^{187}Os/^{188}Os$ while Group I shows low Ru contents and a homogeneous, more radiogenic Os isotopic composition. However there is no correlation between $^{187}Os/^{188}Os$ and Ru (or Pd/Ir, not shown) between or within the two groups.

MSWD = 9.9, 95% confidence level). Compared to other data on chromite-hosted Os-alloys from ophiolites worldwide (Hattori and Hart, 1991; Meibom and Frei, 2002; Meibom et al., 2002, 2004; Malitch, 2004; Walker et al., 2005; Ahmed et al., 2006), the Luobusa Os–Ir alloys define an extremely narrow range of $^{187}Os/^{188}Os$. No correlation is observed between isotopic ratios and Re–PGE abundances or ratios (Fig. 4).

5.2. Dongqiao ophiolite

Group I and Group II alloys in the Dongqiao ophiolite show contrasted $^{187}Os/^{188}Os$ systematics and composition. Group I defines a narrow range of $^{187}Os/^{188}Os$ between 0.1263 to 0.1266 with a weighed average ca. 0.12642 ± 0.00012 (2σ, n = 21, MSWD = 9.6, 95% confidence level); they are indistinguishable from the Luobusa Os alloys in terms of Os-isotope composition. In contrast, Group II shows a much larger range of $^{187}Os/^{188}Os$, from much less radiogenic values ($^{187}Os/^{188}Os$ = 0.1201) up to values similar to those of Group I alloys ($^{187}Os/^{188}Os$ = 0.1264). However, all but one of the grains analyzed from this group have $^{187}Os/^{188}Os$ below 0.1220.

6. Discussion

Group I Os–Ir alloys from the Luobusa and Dongqiao chromitites have an extremely narrow range of Os isotopic composition and similar fractionated PGE patterns. However, in the Dongqiao chromite the Group II alloys show markedly different PGE compositions and Os isotopic characteristics. These features are the key to deciphering the origins of these alloys and of the chromitites.

6.1. The origin of the Os-rich alloys

The origin of primary PGE alloys remains very contentious; because of their intimate relationship with chromite, genetic models must account for the characteristics of both the alloys and the chromite. An overwhelming number of studies have concluded that Os-rich alloys are of magmatic origin. Their association in massive chromite, the common occurrence of typical upper-mantle inclusions (i.e. olivine, pyroxene, sulfide Brenker et al., 2003) or more rarely presumed high-pressure inclusions (Bai et al., 2000), and high-temperature exsolution patterns all argue strongly for a magmatic, i.e. mantle-related, origin. In both the Luobusa and the Dongqiao chromitites, the Os–Ir alloys are enclosed and are rarely connected to fractures. These observations, together with their elemental and isotopic compositions, indicate that they must be considered as primary alloys (i.e. mantle-derived).

Two main hypotheses have been proposed to explain the origin of these Os-rich PGE alloys; either they are formed in the lower mantle (at the core–mantle core transition) or they are the product of much shallower magmatic events, possibly involving H_2O-rich melts (such as boninite) and/or extensive melt–rock reaction in the upper mantle.

The proposal of a deep origin for Ru–Os–Ir-alloys (Bird and Bassett, 1980) is based upon petrological considerations and reports of radiogenic $^{186}Os/^{188}Os$. Extrapolating from the binary phase diagram for Os–Ir, Os–Ru and Ir–Ru (Massalski, 1993) to the ternary Ru–Os–Ir system, an extremely high melting temperature (≥3000 °C) was inferred for such alloys (Bird and Bassett, 1980). "Excess" ^{186}Os has also been reported in Os-rich alloys (Bird et al., 1999; Meibom and Frei, 2002). However, these results have not reproduced (Meibom and Frei, 2002) and alternative models to the outer-core hypothesis (Brandon et al., 2006) have been proposed to produce radiogenic $^{186}Os/^{188}Os$ and $^{187}Os/^{188}Os$ (e.g. (Meibom and Frei, 2002, Brenker et al., 2003)). The analytical methods used in this study do not allow the unambiguous identification of $^{186}Os/^{188}Os$ anomalies. However, the $^{187}Os/^{188}Os$ of the Group I alloys are within the spread of values proposed for the chondritic mantle (see below), ranging from 0.12612 to 0.12672. Furthermore, the Dongqiao Group II alloys display $^{187}Os/^{188}Os$ down to 0.1201, significantly less radiogenic than any reasonable estimate for the convective mantle. Therefore, these alloys apparently were derived from a mantle source without any significant contribution of radiogenic Os from crustal or D" (core–mantle) reservoirs. Furthermore, their $^{187}Os/^{188}Os$ values apparently have not been modified by subsequent processes such as serpentinization, metamorphism, surface transport, sedimentation or weathering during ore formation, as all these processes should result in an increase in $^{187}Os/^{188}Os$.

The PGE characteristics and Os isotopic composition of the various populations of Os-rich alloys in Luobusa and Dongqiao provide several constraints on the processes that led to the formation of these alloys and their host chromitites.

The key characteristics of the Os-rich alloys from these two Tibetan ophiolites are:

1. The occurrence in the Dongqiao podiform chromite of two populations of Os-rich alloys which show distinct PGE compositions and different $^{187}Os/^{188}Os$ systematics;

2. The remarkable isotopic homogeneity of the Group I alloys from both localities;
3. The more scattered Os isotopic composition of Group II alloys and their distinctive pattern.

The occurrence of two populations of Os–Ir-rich alloys characterized by different PGE and $^{187}Os/^{188}Os$ suggests that the two populations were produced by different processes; Group I and Group II Os-rich alloys have sampled different reservoirs or volumes of mantle. The fact that the isotopic and elemental signatures of each population have been preserved suggests that the respective processes and sources were separated in time and/or space and that homogenization/re-equilibration was not possible. Textural and compositional data (Bai et al., 2000) indicate that the alloys were trapped as solids, mainly as individual grains of Os–Ir alloys. Thus they are considered to have formed either prior to, or contemporaneously with, chromite formation (e.g. Bai et al., 2000; Robinson et al., 2004; Malitch, 2004). The remarkable Os-isotope homogeneity of Group I contrasts strongly with the Os isotopic heterogeneity known to be characteristic of the mantle (e.g. Brandon et al., 2000; Alard et al., 2002; Buchl et al., 2004b; Alard et al., 2005) and therefore suggests that extensive melting has taken place in order to collect and isotopically homogenize the Os. Os–Ir grains are devoid of oscillatory zoning, suggesting one "massive" event of Os–Ir-alloy crystallization and thus no possibility for a post-emplacement re-homogenization. The formation of Group I alloys can be explained through the "cluster" model (Tredoux et al., 1995), in which the refractory IPGE remain in the form of metallic clusters during partial melting of the mantle source. These clusters act as nuclei for the early-formed crystals of chromite, when conditions favorable for chromite formation are reached.

The formation of the Ru–Os–Ir alloys will be controlled by the availability of sulfur. Low sulfur fugacity (fS_2) is indicated by the lack of S-bearing alloys (laurite–erlichmanite series, further details are given below). In S-poor environments, the clusters remain free and coalesce to form discrete grains of alloy phases. The Os-isotope composition of Group I alloys ($^{187}Os/^{188}Os = 0.12645 \pm 0.00004$) is similar to that of a broadly chondritic mantle at the time of ophiolite formation (≈ Jurassic). We therefore interpret the Group I alloy phases in the Luobusa and Dongqiao ophiolites as derived from an asthenospheric melt and representing an early cumulate phase of the crystallization of magmas under lithospheric conditions (Ballhaus, 1998; Matveev and Ballhaus, 2002).

6.2. Group II

The Group II alloys have smooth PM-normalized PGE patterns with relative abundances similar to those of residual sulfide in mantle peridotites (Alard, 2000; Lorand and Alard, 2001) and sulfides in abyssal peridotites (Luguet et al., 2001, 2004; Alard et al., 2005). They also show significant isotopic heterogeneity and depleted (unradiogenic) Os compositions (Alard et al., 2005). Whole-rock Re–Os analyses of harzburgites from Dongqiao yield $^{187}Os/^{188}Os$ between 0.1139 and 0.1227 (Zhi et al., 2005) encompassing the range of the Group II alloys reported here. These features strongly suggest that these alloys may represent residual phases from earlier episodes of melt extraction in the mantle protolith.

The presence of these alloys in chromitites that also contain Group I alloys suggests that the Group II alloys can be considered as "xenolithic" in the chromites. In other words, Group II alloys were scavenged from the surrounding oceanic lithospheric mantle during melt–rock reaction. Experimental data show that under low sulfur fugacity (fS_2) the solubility of PGE in sulfide decreases sharply (Peregoedova et al., 2004). Thus as fS_2 decreases, residual MSS will exsolve PGE which will then form discrete alloy phases. The podiform chromitites from both Luobusa and Dongqiao show high Cr#, usually interpreted as indicative of a boninitic melt (Fig. 2), and such melts are S-undersaturated (Keays, 1995).

However, it must be noted that boninites are not the only S-depleted melts; indeed, the solubility of sulfur in basaltic magma increases with decreasing pressure (Mavrogenes and O'Neill, 1999). Thus during its ascent, a magma will become S-deficient, and as it percolates and reacts with the upper mantle, the wall rocks will be stripped of sulfide. Such processes have been suggested to explain the S-(±PGE-) poor compositions of poikiloblastic mantle xenoliths, which show obvious petrographic and geochemical evidence for extensive melt–rock reaction (Lorand and Alard, 2001).

Podiform chromitite bodies commonly are encased in dunite envelopes that grade outward into harzburgite (Zhou et al., 1996; Rollinson, 2005); this is also the case for the Dongqiao and Luobusa ophiolites (Zhou et al., 1996). The systematic association of chromite and dunite suggests that extensive melt–rock reaction occurs during the formation and emplacement of chromite bodies. The REE patterns of both chromitite and the surrounding dunite are characterized by MREE depletion relative to heavy and light REE (Zhou et al., 2005). Such U-shaped REE patterns in dunite have been successfully modeled

as the product of reaction between LREE-enriched magma and peridotites at high melt/rock ratios (Godard et al., 2000; Takazawa et al., 2003).

The olivine saturation of a basaltic liquid will increase as SiO_2 activity ($a[SiO_2]$) falls with decreasing pressure (see Kelemen et al., 1992), so that basaltic liquid during ascent becomes more undersaturated in Opx and S. The dunite-forming reaction consumes orthopyroxene and produces olivine and thus occurs at increasing melt/rock ratios, leading to a further decrease of fS_2. The transition-zone dunites have low Cu and Ni contents, suggesting sulfide removal and further indicating that the melt was S-undersaturated. Thus a large body of evidence strongly suggests that extensive melt–rock reaction plays a key role in the formation and emplacement of podiform chromitites. During this process fS_2 will drop drastically, and the residual sulfide contained in the percolated residue will be transformed into discrete phases such as Ru–Os–Ir alloys and Pt–Fe alloys (Peregoedova et al., 2004).

6.3. Boninite vs tholeiite as the parental magma of chromitite and Os-rich alloys

A boninitic melt does not appear to be an ideal candidate for the source of Group I alloys, for 2 main reasons.

First, the dunitic selvages around the chromitite bodies suggest that the melt had a lower silica activity than the olivine–pyroxene peritectic in the lithospheric wall rocks (Ballhaus, 1998). However, boninite melts are assumed to be generated by shallow melting of a hydrated/metasomatised depleted mantle (e.g. Falloon and Danyushevsky, 2000). The product of such melting will be saturated in Opx (high $a[SiO_2]$) and thus such melts could not produce the typical dunitic envelope through the reaction $Opx + melt_1 \rightarrow Ol + melt_2$. To produce the dunitic selvage, an olivine–saturated melt (low $a[SiO_2]$) is required; such melts are more typical of high-pressure melting of a fertile mantle. Secondly, the "fertile" $^{187}Os/^{188}Os$ composition of Group I alloys is not what would be predicted for the melting of a variably hydrated/metasomatised depleted (harzburgitic) mantle. The Dongqiao harzburgites have yielded unradiogenic Os compositions between 0.1158 and 0.1227 (Zhi et al., 2005). If we assume that these harzburgites are representative of the shallow mantle, i.e. the boninite source, then it is difficult to explain the Os-signature of Type I alloys.

Experimental work shows that in order to have chromite as the only phase on the liquidus, magma mingling between two melts with contrasted silica activity is required (Ballhaus, 1998). The contrast in silica content yields a contrast in viscosity, which delays the complete mixing between the two melts. Chromite then nucleates in the basaltic melt as its interfacial energy is lowest; all excess chromium is quickly concentrated in cumulus chromite, and the high-SiO_2 melt serves only as a diffusion reservoir.

From another perspective, Rollinson (2005) concluded that basaltic melts are capable of crystallizing the low-$Cr^{\#}$ "MORB end-member chromitite" and will evolve through melt–rock reaction into melts with higher $Cr^{\#}$, from which the higher-$Cr^{\#}$ chromites crystallized. The distinctive feature of this model is that the variable chemistry of chromitites in ophiolites is regarded as reflecting a melt that is evolving through a process of melt migration and melt–rock reaction, and does not require a change in the tectonic environment to explain the different chromite types. In this model, the high-$Cr^{\#}$ chromitites can form in the mid-oceanic ridge environment from a tholeiitic melt which then evolves through melt–rock reaction into a high-$a[SiO_2]$ melt similar to boninite. A broadly similar model was proposed to account for the petrogenesis of chromitites with in the Mayari-baracoa ophiolitic belt in Cuba (Proenza et al., 1999). Our data support such a scenario; Group I alloys have $^{187}Os/^{188}Os$ typical of a convective fertile mantle as might be expected of a picritic–tholeitic basalt ($\approx$ "high" pressure melt $\approx$ low $a[SiO_2]$), while Group II have $^{187}Os/^{188}Os$ and PGE relative abundances characteristic of a depleted mantle lithosphere (as now commonly found in abyssal peridotites and ophiolite mantle sections).

Synthesising the data and experimental studies summarized here we can suggest the following tentative scenario: The mantle section of the ophiolite was intensively percolated by a tholeiitic melt (Group I alloys); this melt has low $a[SiO_2]$ and fS_2 (due to the change in pressure on ascent). At the crust–mantle boundary, where magmatic flows diverge, extensive melt–rock reaction takes place (formation of the Moho Transition Zone (MTZ)); the orthopyroxenes of the (metasomatised/hydrated) host harzburgite are dissolved and replaced by olivine. This reaction occurs at increasing melt–rock ratios, so that fS_2 decreases in the surrounding harzburgite (which probably is already depleted in S), forming Group II alloys. Due to this reaction, pools of melt saturated in Opx (high $a[SiO_2]$) and possibly rich in H_2O are isolated. It has been proposed on structural and petrographic grounds and on the basis of Sr and O isotopes (Bosch et al., 2004) that the oceanic hydrothermal system is pervasive down to the MTZ. These results suggest that the ambient mantle at the MTZ is partly

hydrated and thus that water is available for chromite formation (Matveev and Ballhaus, 2002). Mingling between the tholeiitic melt and the locally-produced boninite-like melt triggers the rapid crystallization of chromite. The lack of elemental and isotopic homogenization between the two groups indicates that these processes occurred relatively quickly.

Although there are other lines of evidence for an SSZ environment during the history of these two ophiolites (Massalski, 1993; Zhou et al., 1996), our data do not require such an environment for the genesis of the Os-rich alloys and the crystallization of the host chromitite, which may well predate this stage. The absence of the radiogenic Os isotopic compositions usually taken as characteristic of an SSZ setting (Brandon et al., 1996; Buchl et al., 2002) supports this idea. This hypothesis is also consistent with the most likely model ages deduced for these alloys (ca. 235 Ma; see below) corresponding to stage 1 (MORB-stage) of the ophiolites' evolution.

6.4. Os-isotope constraints on Re–Os evolution models of the convective mantle

The data on the alloy phases in the Tibetan chromitites can be used to constrain the long-term Re–Os evolution of the Earth's upper mantle, because the geological history of the ophiolites is reasonably well-known. Re-depletion model ages are model-dependant, i.e. they depend on the value assigned to the fertile convective mantle. In many cases, Re–Os data from mantle peridotites, especially from Precambrian areas, are referred to a PUM model, with present-day $^{187}Os/^{188}Os = 0.1296 \pm 0.0008$ (Meisel et al., 2001). However, the estimated Os-isotope values of Phanerozoic ophiolitic chromitites worldwide were better fit by the Enstatite Chondrite Reservoir (ECR) model (Walker et al., 2002a; Frei et al., 2005). Recent studies have shown that Enstatite chondrites have an average $^{187}Os/^{188}Os \approx 0.1281 \pm 0.0004$ (Walker et al., 2002b). Yet, the nature of this "late veneer" is extremely contentious and data from various geochemical systems yield (at least at first glance) contradictory conclusions (Drake and Righter, 2002).

The data obtained during this study can be used to further constrain the composition of Earth's mantle. By coupling the Os-isotope composition of Group I alloys and the independent chronological data available for the Luobusa and Dongqiao ophiolites we can distinguish between the various proposed mantle evolution curves (Fig. 5). Given the age constraints, a realistic (see Section 2.1) T_{RD} Os-model age for Group I alloys should be between 90 and 280 Ma. Using an ECR model we obtain T_{RD}^{ECR} for Luobusa and Dongqiao Group I alloys of ca 234 ± 3 Ma and 238 ± 7 Ma, respectively. Note that these model-age uncertainties do not take into account the uncertainty related to the Enstatite Chondrite Re–Os composition. This estimate would agree with the Re–Os isochron age of cumulate gabbroic rocks from the Dongqiao ophiolite c.a. 240 Ma (Zhi

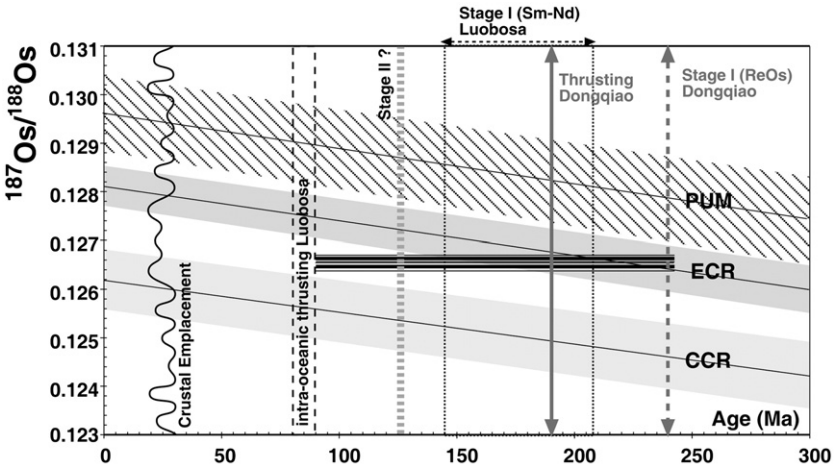

Fig. 5. Models for the Re–Os evolution of the convecting mantle. Mantle evolution curves were defined as follow: CCR (Carbonaceous Chondrite reservoir) curve assumes that the Earth's mantle has an Os isotopic composition and Re/Os similar to that of carbonaceous chondrites ($^{187}Os/^{188}Os_{CC} = 0.1262 \pm 0.0006$, $^{187}Re/^{188}Os_{CC} = 0.392 \pm 0.015$ (Walker et al., 2002b); ECR (Enstatite Chondritic Reservoir) curve is calculated using a present-day $^{187}Os/^{188}Os$ value of 0.1281 ± 0.0004 and $^{187}Re/^{188}Os = 0.421 \pm 0.013$ as measured in enstatite chondrites (Walker et al., 2002b); PUM (Primitive Upper Mantle) curve has a present day $^{187}Os/^{188}Os = 0.1296 \pm 0.0008$ and $^{187}Re/^{188}Os = 0.42$. These estimates were obtained through linear regression through suites of mantle-derived peridotite xenoliths and orogenic-massif peridotites sampling mainly the Proterozoic to Phanerozoic sub-continental upper mantle (Meisel et al., 2001).

et al., unpublished data). In comparison, the PUM model would give mean T_{RD} model ages of ca 440 Ma; these ages are much older than the Neo-Tethys ocean system to which the ophiolites are geologically related. The CCR model yields an unrealistically young age (i.e. $\leq$70 Ma), younger than the age of the ophiolite sole (80–90 Ma). Thus a mantle source for the Group I alloys that has Re–Os characteristics similar within error to the EC model is in agreement with our data.

If we compare our data with previously published ophiolitic datasets that include a significant number of analyzed PGM grains, some similarities in their Os-isotope distributions can be observed (Hattori and Hart, 1991; Meibom and Frei, 2002; Meibom et al., 2002, 2004; Malitch, 2004; Walker et al., 2005). All of these datasets seem to be characterized by two key features (Fig. 6): (*i*) a prominent narrow peak centred around the Os composition of the ECR model at the time of chromite formation (i.e. $\gamma Os_{@t}=0\pm1$) as shown by Group I alloys from Luobusa and Dongqiao. The main exception to this pattern is the Josephine ophiolite, where the main population has a slightly less radiogenic composition ($\gamma Os_{@t}=-2\pm1$); (*ii*) a significant scattering of the data toward unradiogenic (i.e. $\gamma Os_{@t}<-1$) and radiogenic (i.e. $\gamma Os_{@t}>1$) values. We suggest that these scattered data points correspond to "scavenged" alloy grains like the Group II grains from Dongqiao. The remarkable homogeneity of Group I alloys has been interpreted here as the result of the melting and homogenization of large volumes of mantle having a statistically "fertile composition (i.e. the convective upper mantle), whereas Group II alloys are interpreted as residual "lithospheric" sulfides or PGMs. If this scenario can be extended to other localities, as suggested by the distribution of γOs values (Fig. 6), then the mantle source associated with ophiolitic chromitites and their cogenetic PGM seems remarkably homogeneous in term of Os-isotopic composition. This homogeneity could result either from the convective mixing effect or to an averaging of large volumes during the melting process.

6.5. Relict sub-continental lithosphere in the Dongqiao ophiolite

The wide scatter of the $^{187}Os/^{188}Os$ of the Ru–Os–Ir alloys from the Dongqiao ophiolitic podiform chromitite (0.12003–0.12664, $n=27$; see Table 2) provides evidence that the Ru–Os–Ir alloys record much older melting events than would be expected from a single-stage melting of undepleted mantle. The Group II alloys in the Dongqiao ophiolite show ECR model ages ranging from 850 to 1140 Ma. These ages demonstrate that the Os-rich alloys encapsulated in the refractory chromite grains can indeed remain isolated from Os-isotopic equilibration under mantle conditions, and imply that residual mantle sections of ophiolites can preserve compositional heterogeneities for at least 0.9 Ga, if the alloys are protected by chromite. The older T_{RD} model ages of the Group II alloys suggest that the ophiolite had a Precambrian mantle precursor, which experienced melting events during Late Proterozoic time. T_{RD} whole-rock model ages of 1436 and 2005 Ma have been reported for Dongqiao harzburgites (Zhi

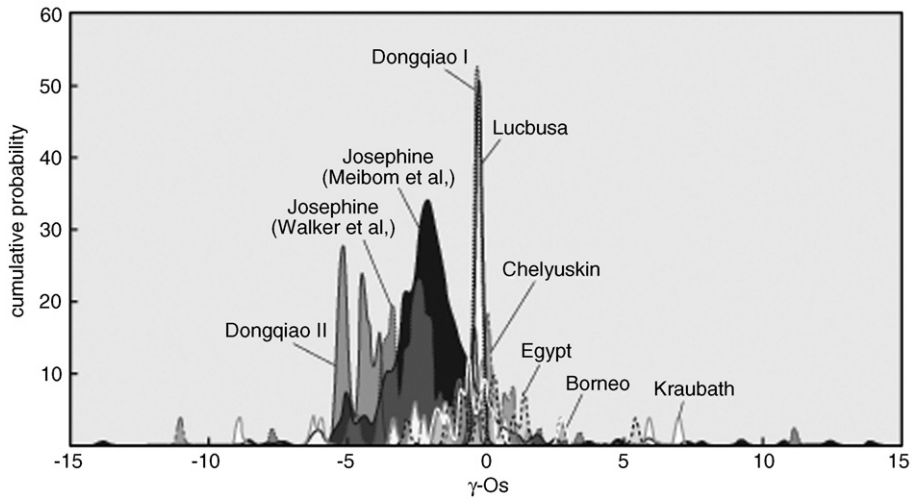

Fig. 6. Cumulative probability plot of $\gamma Os_{@t}$ (calculated relative to an ECR model) for PGE alloy grains from ophiolites world-wide. Data from (Hattori and Hart, 1991; Meibom and Frei, 2002; Meibom et al., 2002, 2004; Malitch, 2004; Walker et al., 2005; Ahmed et al., 2006).

et al., 2005). Therefore the Os-isotope compositions of both Group II alloys and the harzburgites suggest that the Dongqiao ophiolite may contain ancient mantle components, predating by at least 1 Ga the formation of the MORB type magmas. In effect, a fragment of ancient sub-continental lithosphere became part of the ocean basin and served as the basement for the accumulation of oceanic basalts and sediments.

An analogous evolution from sub-continental lithospheric mantle to oceanic mantle has been described in the westernmost part of the Tethyan chain, in the ophiolites of the Internal Ligurides. It has been proposed that pre-Jurassic lithospheric mantle was unroofed by detachment of the continental crust, and that this mantle was subsequently intruded by oceanic basalts, which ultimately formed a typical oceanic volcanic-sedimentary section overlying the peridotitic mantle (Rampone et al., 2005). This model is supported by the $^{187}Os/^{188}Os$ values of the Internal Liguride ophiolitic peridotites, which range from 0.1219 to 0.1252 ($n=5$, (Snow et al., 2000)), recording ancient mantle melting in the Neo-Tethyan ophiolite. *In situ* Os isotopic studies of the primary magmatic sulfides in these rocks has yielded $^{187}Os/^{188}Os$ as low as 0.111, which correspond to T_{RD} ages of ca 2.39 Ga (Alard et al., 2005).

A similar unroofing of continental mantle may be recorded in the Svecofennian (1.95 Ga) Jormua ophiolite (Finland), where an Archean SCLM was exposed during the early stages of Svecofennian ocean formation (Peltonen et al., 2003); a thick Svecofennian volcanic-sedimentary sequence was deposited on the mantle substrate prior to the obduction of the ophiolitic sequence. In the Jormua ophiolite, the large negative γOs value (−5.1 at 1.95 Ga) for oxides separated from serpentinites, and for the whole rock serpentinites, is most consistent with derivation from ancient SCLM that had experienced major loss of Re during a much earlier melt extraction event. Their T_{RD} is about 2.9 Ga; this is consistent with the 3.1 Ga age of the Baltic Shield lithospheric mantle in this area, as recorded by Archean zircons captured in the ophiolitic cumulate clinopyroxenite (Peltonen et al., 2003). This is probably the earliest possible time at which substantial Re could have been removed from this mantle.

Ancient melting events also are recorded in mantle peridotites from other oceanic environments. The "future" SSZ-type ophiolitic mantle peridotite from the Izu–Bonin–Mariana forearc in the western Pacific Ocean (Parkinson et al., 1998), and peridotite xenoliths from the Kerguelen Islands in the southern Indian Ocean (Hassler and Shimizu, 1998), have modern $^{187}Os/^{188}Os$ as low as 0.119. These depleted compositions have been interpreted to reflect either derivation from sub-continental lithospheric mantle detached from cratons (Hassler and Shimizu, 1998) or Re-depleted reservoirs that have survived within the oceanic mantle for >1 Ga (Parkinson et al., 1998). Recently, magmatic sulfides, either hosted in Opx or occurring as relicts within abyssal serpentinites from the MAR and the SWIR, have yielded T_{RD} ages in excess of 2.2 Ga (Alard et al., 2005).

7. Conclusions

Two populations of Os-rich alloys have been recognized in the Luobusa and Dongqiao ophiolites; their distinct elemental and isotopic compositions indicate that they are from different sources and were produced by different processes. This suggests that chromitites and their host Os-rich alloys were produced by 2 episodes separated in time and space. Group I alloys from both localities show a narrow range of $^{187}Os/^{188}Os$, suggesting that the parental melts of the podiform chromitites were derived from a relatively homogeneous fertile asthenospheric mantle. Group II alloys from the Dongqiao ophiolite show "smooth" PGE-patterns reminiscent of residual sulfide, and have much more scattered and less radiogenic Os isotopic compositions, suggesting that they were derived from the breakdown of residual sulfides during melt–rock reaction, a process which is now seen as characteristic of the shallow oceanic harzburgitic mantle.

The Group II alloys from the Dongqiao ophiolite define old melting events, and suggest that the Neo-Tethyan oceanic mantle contained relicts of sub-continental lithospheric mantle that experienced melt extraction at least 1 Ga before it was affected by the percolation of MORB type melt.

The presence of these two groups of alloys in a single chromitite sample suggests that mingling between asthenospheric and older lithospheric Os occurred and is probably responsible for the isotopic heterogeneity observed in whole-rock studies of the chromitites in the Luobusa and Dongqiao ophiolites (Zhi et al., in preparation). This mechanism may also explain the Os-isotope heterogeneity found in chromitites from other ophiolites (e.g. Troodos (Buchl et al., 2004a), Cuba (Frei et al., 2005; Gervilla et al., 2005)). This situation would be exacerbated if the harzburgite had been extensively metasomatised and thus contained different generations of sulfides, as found in abyssal peridotites (Alard et al., 2005). The occurrence of several PGM populations also explains the peculiar $^{187}Os/^{188}Os$ distribution found in ophiolitic chromitites world-wide (Hattori and Hart, 1991; Meibom and Frei,

2002; Meibom et al., 2002, 2004; Malitch, 2004; Walker et al., 2005). These observations suggest that the separation and *in situ* analysis of Os-rich alloys (majors, traces and isotopes) in chromitites may provide an ideal tool to study the evolution of the deep (magma source) and shallow oceanic mantle, and thus provide robust estimates of the $^{187}Os/^{188}Os$ of the oceanic asthenosphere through time.

Our data provide further support for an ECR-like Os-isotope evolution for the convective oceanic mantle (Walker et al., 2002a). This estimate is significantly less radiogenic than the PUM and more radiogenic than the DMM. The primitive nature of the PUM is debatable, and in our view highly unlikely. It has been derived by regression through data from xenolith suites and peridotite massifs, sampling mainly sub-continental lithospheric mantle of Proterozoic to Phanerozoic age (Meisel et al., 2001) and is more likely to represent a metasomatised lithospheric mantle (Alard et al., 2002). The present study suggests that its Os-isotope composition and evolution have little in common with the source of the ophiolitic chromitites (assumed to be the convecting asthenospheric mantle) (cf Walker et al., 2002a). Although the DMM estimate is loosely constrained our data suggest that the source of the chromitites is not well characterized by the DMM model.

Acknowledgements

This work was supported by the National Natural Science Foundation of China (Grant Nos. 40572036, 40610104005, 40672051 and 40473008) and ARC Discovery and Linkage International Grants (SYO'R and WLG). Analytical data were obtained using instrumentation funded by ARC LIEF, and DEST Systemic Infrastructure Grants and Macquarie University. This is contribution 482 from the ARC National Key Centre for Geochemical Evolution and Metallogeny of Continents (www.es.mq.edu.au/GEMOC). Special thanks go to Prof. W.J. Bai and Q.S. Fang working in the Institute of Geology, CAGS, Beijing, China for providing the Os-rich alloy samples for this study. We also thank Professor Robert Frei and another reviewer for their insightful reviews of the manuscript, which helped greatly to improve its quality clarity, and we specially thank Professor Rick Carlson for his editorial handling.

Appendix A. Supplementary data

Supplementary data associated with this article can be found, in the online version, at doi:10.1016/j.epsl.2007.05.044.

References

Ahmed, A.H., Hanghøj, K., Kelemen, P.B., Hart, S.R., Arai, S., 2006. Osmium isotope systematics of the Proterozoic and Phanerozoic ophiolitic chromitites: in-situ ion probe analysis of primary Os-rich PGM. Earth Planet. Sci. Lett. 245, 777–791.

Alard, O., 2000. Chalcophile and siderophile elements in the mantle: geochemical characteristics and distributions, Ph.D., Macquarie University.

Alard, O., Griffin, W.L., Pearson, N.J., Lorand, J.-P., O'Reilly, S.Y., 2002. New insights into the Re–Os systematics of sub-continental lithospheric mantle from in situ analysis of sulphides. Earth Planet. Sci. Lett. 203, 651–663.

Alard, O., Luguet, A., Pearson, N.J., Griffin, W.L., Lorand, J.-P., Gannoun, A., Burton, K.W., O'Reilly, S.Y., 2005. In-situ Os isotopes in abyssal peridotites bridge the isotopic-gap between MORBs and their source mantle. Nature 436, 1005–1008.

Allègre, C.J., Courtillot, V., Mattauer, M., Tapponnier, P.A., Mattauer, H.M., Coulon, C., Jaeger, J.J., Achache, J., Schärer, U., Marcoux, J., Burg, J.P., Girardeau, J., Armijo, R., 1984. Structure and evolution of the Himalaya–Tibet orogenic belt. Nature 307, 17–22.

Bai, W.J., Robinson, P.T., Fang, Q.S., Yang, J.S., Yan, B.G., Zhang, Z.M., Hu, X.F., Zhou, M.F., Malpas, J., 2000. The PGE and base-mental alloys in the podiform chromitite of the Luobusa ophiolite, Southern Tibet. Can. J. Earth Sci. 38, 585–598.

Ballhaus, C., 1998. Origin of podiform chromite deposits by magma mingling. Earth Planet. Sci. Lett. 156, 185–193.

Bird, J.M., Bassett, W.A., 1980. Evidence of a deep mantle history in terrestrial osmium–iridium–ruthenium alloys. J. Geophys. Res. 85, 2012–2019.

Bird, J.M., Meibom, A., Frei, R., Nagler, T.F., 1999. Osmium and lead isotopes of rare OsIrRu minerals: derivation from the core–mantle boundary region? Earth Planet. Sci. Lett. 170, 83–92.

Bosch, D., Jamais, M., Boudier, F., Nicolas, A., Dautria, J.-M., Agrinier, P., 2004. Deep and high-temperature hydrothermal circulation in the Oman ophiolite — petrological and isotopic evidence. J. Petrol. 45, 1181–1208.

Brandon, A.D., Creaser, R.A., Shirey, S.B., Carlson, R.W., 1996. Osmium recycling in subduction zones. Science 272, 861–864.

Brandon, A.D., Snow, J.E., Walker, R.J., Morgan, J.W., Mock, T.D., 2000. ^{190}Pt–^{186}Os and ^{187}Re–^{187}Os systematics of abyssal peridotites. Earth Planet. Sci. Lett. 177, 319–335.

Brandon, A.D., Walker, R.J., Puchtel, I.S., 2006. Platinum–osmium isotope evolution of the Earth's mantle: constraints from chondrites and Os-rich alloys. Geochim. Cosmochim. Acta 70, 2093–2103.

Brenker, F.E., Meibom, A., Frei, R., 2003. On the formation of peridotite-derived Os-rich PGE alloys. Am. Mineral. 88, 1731–1740.

Buchl, A., Brugmann, G., Batanova, V.G., Munker, C., Hofmann, A.W., 2002. Melt percolation monitored by Os isotopes and HSE abundances: a case study from the mantle section of the Troodos Ophiolite. Earth Planet. Sci. Lett. 204, 385–402.

Buchl, A., Brugmann, G., Batanova, V.G., 2004a. Formation of podiform chromitite deposits: implications from PGE abundances and Os isotopic compositions of chromites from the Troodos complex, Cyprus. Chem. Geol. 208, 217–232.

Buchl, A., Brugmann, G.E., Batanova, V.G., Hofmann, A.W., 2004b. Os mobilization during melt percolation: the evolution of Os isotope heterogeneities in the mantle sequence of the Troodos ophiolite, Cyprus. Geochim. Cosmochim. Acta 68, 3397–3408.

Dick, H.J.B., Bullen, T., 1984. Chrominium spinel as a petrogenetic indicator in abyssal and alpine-type peridotites and spatially associated lavas. Contrib. Mineral. Petrol. 86, 54–76.

Drake, M.J., Righter, K., 2002. Determining the composition of the Earth. Nature 416, 39–43.

Falloon, T.J., Danyushevsky, L.V., 2000. Melting of Refractory mantle at 1.5–2 and 2.5 GPa under anhydrous condition and H2O-undersaturated conditions: implications for the petrogenesis of high-Ca boninites and the influence of subduction components on mantle meltings. J. Petrol. 41, 257–283.

Frei, R., Gervilla, F., Meibom, A., Proenza, J., Garrido, C.J., 2005. Os isotope heterogeneity of the upper mantle: evidence from the Mayarı–Baracoa ophiolite belt in eastern Cuba. Earth Planet. Sci. Lett. 241, 466–476.

Gervilla, F., Proenza, J.A., Frei, R., Gonzalez-Jiménez, J.M., Garrido, C.J., Melgarejo, J.C., Meibom, A., Diaz-Martinez, R., Lavaut, W., 2005. Distribution of platinum-group elements and Os isotopes in chromite ores from Meyarí–Baracoa Ophiolitic belt (eastern Cuba). Contrib. Mineral. Petrol. 150, 589–607.

Godard, M., Jousselin, D., Bodinier, J.L., 2000. Relationships between geochemistry and structure beneath a palaeo-spreading centre: a study of the mantle section in the Oman ophiolite. Earth Planet. Sci. Lett. 180, 133–148.

Harris, D.C., Cabri, L.J., 1991. Nomenclature of platinum group-element alloys: review and revision. Can. Miner 29, 231–237.

Hassler, D.R., Shimizu, N., 1998. Osmium isotopic evidence for ancient subcontinental lithospheric mantle beneath the Kerguelen Islands, Southern Indian Ocean. Science 280, 418–421.

Hattori, K., Hart, S.R., 1991. Osmium-isotope ratios of platinum group mineral associated with ultramafic inclusions; Os isotopic evolution of the oceanic mantle. Earth Planet. Sci. Lett. 107, 499–514.

Keays, R.R., 1995. The role of komatiitic and picritic magmatism and S-saturation in the formation of ore deposits. Lithos 34, 1–18.

Kelemen, P.B., Dick, H.J.B., Quick, J.E., 1992. Formation of harzburgite by pervasive melt/rock reaction in the upper mantle. Nature 358, 635–641.

Lago, B.L., Rabinowicz, M., Nicolas, A., 1982. Podiform chromite ore bodies. A genetic model. J. Petrol. 23, 103–125.

Lorand, J.-P., Alard, O., 2001. Platinum-group element abundances in the upper mantle: new constraints from in situ and whole-rock analyses of Massif Central xenoliths (France). Geochim. Cosmochim. Acta 65, 2789–2806.

Luguet, A., Alard, O., Lorand, J.P., Pearson, N.J., Ryan, C., O'Reilly, S.Y., 2001. Laser-ablation microprobe (LAM)-ICPMS unravels the highly siderophile element geochemistry of the oceanic mantle. Earth Planet. Sci. Lett. 189, 285–294.

Luguet, A., Lorand, J.-P., Alard, O., Cottin, J.-Y., 2004. A multi-technique study of platinum-group elements systematic in some ligurian ophiolitic peridotites. Chem. Geol. 208, 175–194.

Malitch, K.N., 2004. Osmium isotope constraints on contrasting sources and prolonged melting in the proterozoic upper mantle: evidence from ophiolitic Ru–Os sulfides and Ru–Os–Ir alloys. Chem. Geol. 208, 157–173.

Malpas, J., Zhou, M.F., Robinson, P.T., Reynolds, P., 2003. Geochemical and geochronological constraints on the origin and emplacement of the Yarlung–Zangbo ophiolites, Southern Tibet. In: Dilek, Y., Robinson, P.T. (Eds.), Ophiolites in Earth History Special Publications, vol. 218. Geological Society, London, pp. 191–206.

Massalski, T.B., 1993. Binary Alloy Phase Diagrams Amer. Soc., Metals Park. Ohio. 2224 pp.

Matveev, S., Ballhaus, C., 2002. Role of water in the origin of podiform chromitite deposits. Earth Planet. Sci. Lett. 203, 235–243.

Mavrogenes, J.A., O'Neill, H.S.C., 1999. The relative effects of pressure, temperature and oxygen fugacity on the solubility of sulfide in mafic magmas. Geochim. Cosmochim. Acta 63, 1173–1180.

Meibom, A., Frei, R., 2002. Evidence for an ancient osmium isotopic reservoir in Earth. Science 296, 516–518.

Meibom, A., Sleep, N.H., Chamberlain, C.P., Coleman, R.G., Frei, R., Hren, M.T., Wooden, J.L., 2002. Re–Os isotope evidence for long lived heterogeneity and equilibrium processes in Earth's upper mantle. Nature 410, 705–708.

Meibom, A., Frei, R., Sleep, N.H., 2004. Osmium isotopic compositions of Os-rich platinum group element alloys from the Klamath and Siskiyou Mountains. J. Geophys. Res., [Solid Earth] 109 art. no.-B02203.

Meisel, T., Walker, R.J., Irving, A.J., Lorand, J.-P., 2001. Osmium isotopic compositions of mantle xenoliths: a global perspective. Geochim. Cosmochim. Acta 65, 1311–1323.

Parkinson, I.J., Hawkesworth, C.J., Cohen, A.S., 1998. Ancient mantle in a modern arc: osmium isotopes in Izu–Bonin–Mariana forearc peridotites. Science 281, 2011–2013.

Pearson, N.J., Alard, O., Griffin, W.L., Jackson, S.E., O'Reilly, S.Y., 2002. In situ measurement of Re–Os isotopes in mantle sulfides by laser ablation multicollector-inductively coupled plasma mass spectrometry: analytical methods and preliminary results. Geochim. Cosmochim. Acta 66, 1037–1050.

Peltonen, P., Manttani, I., Huhma, H., Kontinen, A., 2003. Archean zircons from the mantle: the Jormua ophiolite revisited. Geology 31, 645–648.

Peregoedova, A., Barnes, S.J., Baker, D.R., 2004. The formation of Pt–Ir alloys and Cu–Pd-rich sulfide melts by partial desulfurization of Fe–Ni–Cu sulfides: results of experiments and implications for natural systems. Chem. Geol. 208, 247–264.

Proenza, J., Gervilla, F., Melgarejo, J.C., Bodinier, J.L., 1999. Al-and Cr-rich chromitites from the Mayari–Baracoa ophiolitic belt (Eastern Cuba): consequence of interaction between volatile-rich melts and peridotites in suprasubduction mantle. Econ. Geol. 94, 547–566.

Rampone, E., Romairone, A., Abouchami, W., Piccardo, G.B., Hofmann, A.W., 2005. Chronology, petrology and isotope geochemistry of the Erro-Tobbio peridotites (Ligurian Alps, Italy): record of late Palaezoic Lithospheric Extension. J. Petrol. 46, 799–827.

Robinson, P.T., Bai, W.J., Malpas, J., Yang, J.S., Zhou, M.F., Fang, Q.S., Hu, X.F., Cameron, S., Staudigel, H., 2004. Ultra-high pressure minerals in the Luobusa ophiolite, Tibet, and their tectonic implications. In: Malpas, J., Fletcher, C.J.N., Ali, J.R., Aitchison, J.C. (Eds.), Aspects of the Tectonic Evolution of China Special Publications, vol. 226. Geological Society, London, pp. 247–271.

Rollinson, H., 2005. Chromite in the mantle section of the Oman ophiolite: a new genetic model. The Island Arc 14, 542–550.

Sengor, A.M.C., 1984. The Cimmerides of Eastern Asia: history of the eastern end of Paleo-Tethys. Geol. Soc. France Mem. N. S. 147, 139–167.

Snow, J.E., Schmidt, G., Rampone, E., 2000. Os isotopes and highly siderophile elements (HSE) in the Ligurian ophiolites, Italy. Earth Planet. Sci. Lett. 175, 119–132.

Takazawa, E., Frey, F.A., Shimizu, N., Obata, M., Bodinier, J.L., 2003. Spatial variation of trace element abundances in clinopyroxenes from the layered orogenic lherzolite (Horoman peridotite, Japan): implications for melt flow and reaction in the upper mantle. Geochim. Cosmochim. Acta 67, A471.

Tredoux, M., Lindsay, N.M., Davies, G., McDonald, I., 1995. The fractionation of platinum-group elements in magmatic systems, with the suggestion of a novel casual mechanism. S. Afr. J. Geol. 98, 157–167.

Walker, R.J., Prichard, H.M., Ishiwatari, A., Pimentel, M., 2002a. The osmium isotopic composition of convecting upper mantle deduced

from ophiolite chromites. Geochim. Cosmochim. Acta 66, 329–345.

Walker, R.J., Horan, M.F., Morgan, J.W., Becker, H., Grossman, J.N., Rubin, A.E., 2002b. Comparative ^{187}Re–^{187}Os systematics of chondrites: implications regarding early solar system processes. Geochim. Cosmochim. Acta 66, 4187–4201.

Walker, R.J., Brandon, A.D., Bird, J.M., Piccoli, P.M., McDonough, W.F., Ash, R.D., 2005. ^{187}Os–^{186}Os systematics of Os–Ir–Ru alloy grains from Southwestern Oregon. Earth Planet. Sci. Lett. 230, 221–226.

Zhi, X.C. Shi, R.D., Jin, Z.M., Xia, Q.X., Wang, Y.F., in preparation. Re-Os isotope systematics of the Dongqiao Neo-Tethys ophiolite, northern Tibet.

Zhi, X.C., X.Q.A., Wang, Y.F., 2005. Re–Os isotopic systematic of the Neo-Tethys Dongqiao Ophiolite Complex. Northern Tibet: First Data, 15th Annual V.M. Goldschmidt Conference, Moscow, Idaho, U.S.A. , p. A286.

Zhou, M.-F., Robinson, P.T., Malpas, J., Li, Z., 1996. Podiform chromites in the Luobusa Ophiolite (southern Tibet): implications for melt–rock interaction and chromite segregation in the upper mantle. J. Petrol. 37, 3–21.

Zhou, M.F., Malpas, J., Robinson, P.T., Reynolds, P., 1997. The dynamothermal aureole of the Dongqiao ophiolite, northern Tibet. Can. J. Earth Sci. 34, 59–65.

Zhou, S., Mo, X.X., Mahoney, J.J., Zhang, S.Q., Guo, T.Y., Zhao, Z.D., 2002. Geochronology and Nd and Pb isotope characteristics of gabbro dikes in the Luobusa ophiolite, Tibet. Chin. Sci. Bull. 47, 143–146.

Zhou, M.F., Robinson, P.T., Malpas, J., Edwards, S.J., Qi, L., 2005. REE and PGE geochemical constraints on the formation of dunites in the Luobusa ophiolite, Southern Tibet. J. Petrol. 46, 615–639.